

A Frustrated 3-Dimensional Antiferromagnet: Stacked $J_1 - J_2$ Layers

Onofre Rojas*, C. J. Hamer and J. Oitmaa

School of Physics, The University of New South Wales, Sydney 2052, Australia.

We study a frustrated 3D antiferromagnet of stacked $J_1 - J_2$ layers. The intermediate ‘quantum spin liquid’ phase, present in the 2D case, narrows with increasing interlayer coupling and vanishes at a triple point. Beyond this there is a direct first-order transition from Néel to columnar order. Possible applications to real materials are discussed.

PACS numbers: PACS Indices: 05.30.-d,75.10.-b,75.10.Jm,75.30.Ds,75.30.Kz

(Submitted to Phys. Rev. B)

I. INTRODUCTION

The study of frustrated quantum antiferromagnets remains an active field, characterized by strong interplay between theory and experiment. A model which has been studied extensively (see [1–15] and references therein) is the so called ‘ $J_1 - J_2$ model’, a spin-1/2 system on the two dimensional square lattice with nearest and next-nearest neighbor interactions of strength J_1 and J_2 respectively, both being antiferromagnetic. The Néel order at $T = 0$, which pertains for $J_2 = 0$, is destabilized by the frustrating J_2 interaction and vanishes at around $J_2/J_1 \simeq 0.4$. In the opposite limit, of large J_2 , a columnar (often ambiguously termed ‘collinear’) ordered phase occurs, in which successive columns (or rows) of spins alternate in direction. The columnar phase becomes unstable at $J_2/J_1 \simeq 0.6$. A magnetically disordered region thus exists in the region $0.4 \lesssim J_2/J_1 \lesssim 0.6$, the nature of which remains not fully resolved.

It is of interest to ask what happens to this intermediate phase, and indeed to the entire phase diagram, when these $J_1 - J_2$ layers are coupled, perhaps weakly, in the third direction, forming a 3-dimensional structure. This is the main topic of this paper. It has already been studied by Schmalfuss *et al.* [16] using the coupled-cluster and rotation-invariant Green’s function methods. They found that the disordered region becomes narrower as a function of J_2 when J_3 is increased, and vanishes entirely at $J_3/J_1 \simeq 0.2 - 0.3$. We will address the question using series expansion methods [17] in both Néel and columnar phases, as well as first order spin-wave theory.

It has been argued recently that the layered materials $\text{Li}_2\text{VO}_2\text{SiO}_4$, $\text{Li}_2\text{VOGeO}_4$ are well represented by the spin-1/2 $J_1 - J_2$ model with $J_2 \gg J_1$, i.e. in the columnar phase. In ref. [18] high-temperature expansions for the specific heat and magnetic susceptibility for the purely 2-d model were used to try to constrain the values of the exchange parameters by fitting to the experimental data. At the same time an *ab initio* local density approxima-

tion (LDA) calculation of the exchange parameters J_1 , J_2 , J_3 yielded (0.75K, 8.8K, 0.25K) for the Si material and (1.7K, 8.1K, 0.19K) for the Ge system. This suggests that the coupling in the third direction is by no means negligible and ought to be included in a fitting procedure.

We mention also that a popular, though not universally accepted, scenario to understand the magnetic properties of the recently discovered superconducting iron pnictides is via a spin-1 layered $J_1 - J_2$ model [19, 20]. While we do not consider these systems explicitly here, our results may have some relevance.

Our model is a 3-dimensional spin-1/2 antiferromagnet, on a tetragonal lattice, as shown in Figure 1(a). Frustrating J_2 interactions occur in the x-y plane but not in the third direction. All interactions are antiferromagnetic.

The Hamiltonian, in standard notation, is

$$H = J_1 \sum_{\langle ij \rangle}^{(1)} \mathbf{S}_i \cdot \mathbf{S}_j + J_2 \sum_{\langle ik \rangle}^{(2)} \mathbf{S}_i \cdot \mathbf{S}_k + J_1 \sum_{\langle il \rangle}^{(3)} \mathbf{S}_i \cdot \mathbf{S}_l \quad (1)$$

where the summations are over the three classes of coupling respectively.

In the following section, section II, we present our zero temperature calculations and results, for the ground state energy and sublattice magnetization (order parameter), for both the Néel and columnar phases. Our results support a phase diagram of the form shown in Figure 1(b), and we estimate the location of the triple point at $J_2/J_1 = 0.54(3)$ and $J_3/J_1 = 0.16(3)$. Our series results are compared with the results of linear spin-wave theory. In section III we use series methods to compute the 1-magnon dispersion curves, in both ordered phases, and again compare our results with the spin-wave predictions. The spin-wave theory follows standard lines and, for completeness, is outlined in the appendix. In section IV we present our conclusions and discussion.

II. GROUND STATE BULK PROPERTIES

The series expansion method is based on perturbative calculations for a sequence of finite connected clusters,

*Departamento de Ciências Exatas, Universidade Federal de Lavras, CP 3037, 37200-000, Lavras, MG, Brazil.

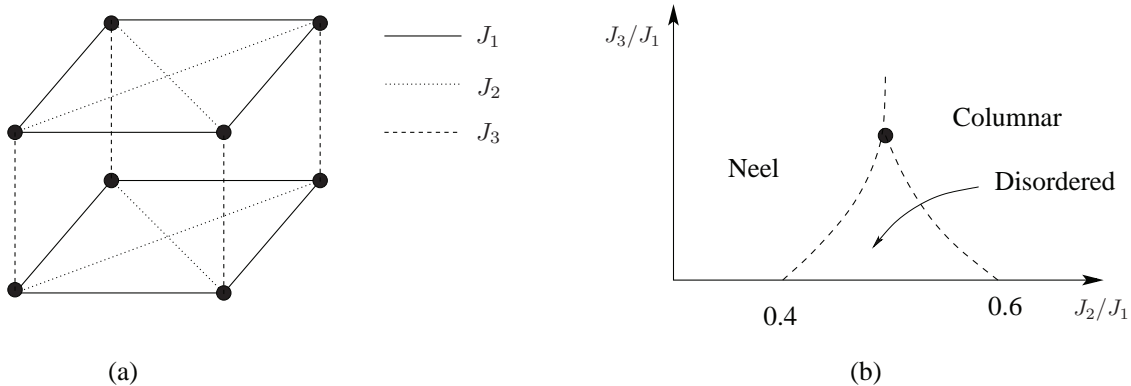


Figure 1: (a) Tetragonal unit cell of the model; (b) Conjectured phase diagram of the model at $T = 0$. The transition lines are (probably) first-order and the solid circle is thus a triple point.

which are then combined to obtain a series for the bulk system. In practice it is possible to treat of order 10^6 different clusters and to obtain series of order 10-20 terms, depending on the model. The Hamiltonian is written in the standard form $H = H_0 + \lambda V$ where H_0 has a simple known ground state. In the present work we use an Ising expansion in which H_0 consists of the diagonal $S_i^z S_j^z$ terms and the quantum fluctuations are included in the perturbation V . Series are obtained in powers of λ , and extrapolated to $\lambda = 1$ via standard Padé or differential approximant methods. The interested reader is referred to the book [17] for more detail.

A. Néel Phase

It is well known that the unfrustrated square lattice ($J_2 = J_3 = 0$) has reduced Néel order in the ground

state. This is a 2-sublattice structure with spins pointing in opposite directions on the two sublattices. For technical reasons it is useful to perform a spin rotation on the B sublattice, making the unperturbed ground state ferromagnetic. The Hamiltonian, for a lattice of N sites is then written as

$$H = -\frac{1}{4}(2J_1 - 2J_2 + J_3)N + H_0 + \lambda V \quad (2)$$

with

$$H_0 = J_1 \sum_{\langle ij \rangle}^{(1)} \left(\frac{1}{4} - S_i^z S_j^z \right) + J_2 \sum_{\langle ik \rangle}^{(2)} \left(S_i^z S_k^z - \frac{1}{4} \right) + J_3 \sum_{\langle il \rangle}^{(3)} \left(\frac{1}{4} - S_i^z S_l^z \right) \quad (3)$$

$$V = \frac{1}{2} J_1 \sum_{\langle ij \rangle}^{(1)} (S_i^+ S_j^+ + S_i^- S_j^-) + \frac{1}{2} J_2 \sum_{\langle ik \rangle}^{(2)} (S_i^+ S_k^- + S_i^- S_k^+) + \frac{1}{2} J_3 \sum_{\langle il \rangle}^{(3)} (S_i^+ S_l^+ + S_i^- S_l^-) \quad (4)$$

We have added and subtracted constant terms to make the unperturbed energy zero.

We have obtained series for the ground state energy E_0 and the magnetization M to order λ^9 . The rapid proliferation of clusters with 3 bond types (there are 320274 with 9 or fewer sites) limits the length of the series ob-

tainable. The data are far too extensive to present, but can be provided on request. The values of E_0 and M can then be estimated, with some uncertainty, for any values of J_2 and J_3 . It is convenient to set $J_1 = 1$ to set the energy scale. A display of the results is deferred to the third subsection, where they are presented together with

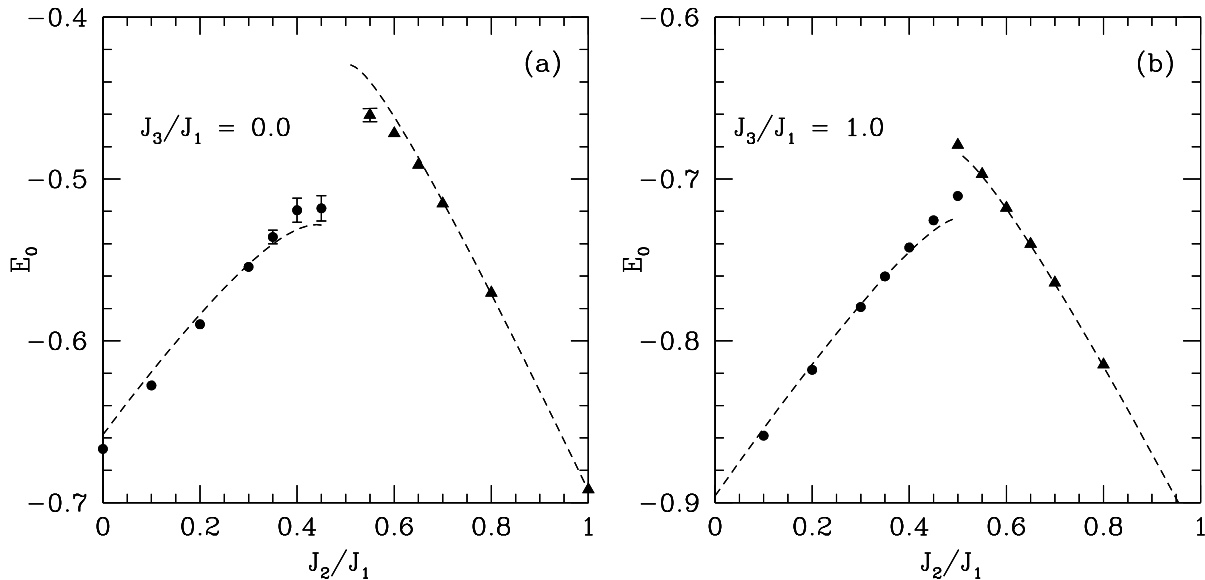


Figure 2: Series estimates of the ground-state energy per site at couplings (a) $J_3/J_1 = 0.0$, (b) $J_3/J_1 = 1.0$. Filled circles - Néel phase; filled triangles - columnar phase. The dashed lines are linear spin-wave predictions in each phase.

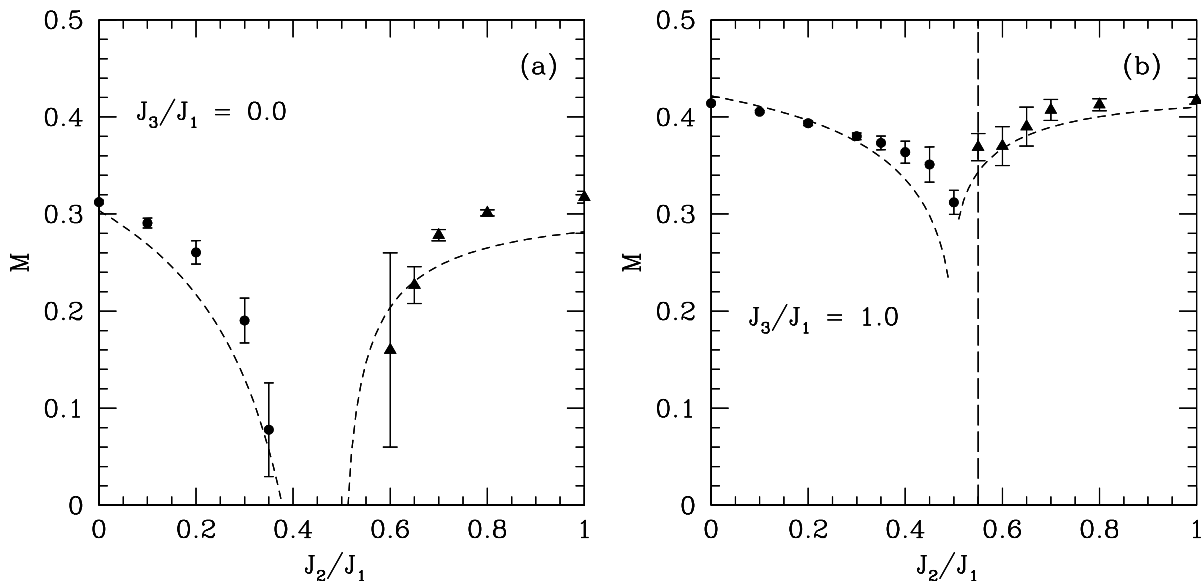


Figure 3: Series estimates of the staggered magnetizations in each phase at couplings (a) $J_3/J_1 = 0.0$, (b) $J_3/J_1 = 1.0$. Filled circles - Néel phase; filled triangles - columnar phase. The dashed curves are linear spin-wave predictions in each phase. The dashed vertical line in Figure 3b marks the estimated position of the first-order transition.

the results for the columnar phase.

B. Columnar Phase

In the columnar phase the spins on alternating columns in a particular x-y plane will point in opposite directions. This satisfies all of the strong J_2 bonds but leaves half

of the J_1 bonds frustrated. In adjacent planes these are shifted by one lattice spacing, leaving all of the J_3 bonds satisfied. This structure has an additional 2-fold degeneracy as columns can equally well be ‘rows’. Again it is convenient to carry out a spin rotation on ‘down’ sites, yielding

with

$$H = -\frac{1}{4}(2J_2 + J_3)N + H_0 + \lambda V \quad (5)$$

$$H_0 = J_1 \sum_{\langle ij \rangle}^{(1x)} \left(\frac{1}{4} - S_i^z S_j^z \right) + J_1 \sum_{\langle ij \rangle}^{(1y)} \left(S_i^z S_j^z - \frac{1}{4} \right) + J_2 \sum_{\langle ik \rangle}^{(2)} \left(\frac{1}{4} - S_i^z S_k^z \right) + J_3 \sum_{\langle il \rangle}^{(3)} \left(\frac{1}{4} - S_i^z S_l^z \right) \quad (6)$$

$$V = \frac{1}{2} J_1 \sum_{\langle ij \rangle}^{(1x)} (S_i^+ S_j^+ + S_i^- S_j^-) + \frac{1}{2} J_1 \sum_{\langle ij \rangle}^{(1y)} (S_i^+ S_j^- + S_i^- S_j^+) \\ + \frac{1}{2} J_2 \sum_{\langle ik \rangle}^{(2)} (S_i^+ S_k^- + S_i^- S_k^+) + \frac{1}{2} J_3 \sum_{\langle il \rangle}^{(3)} (S_i^+ S_l^+ + S_i^- S_l^-) \quad (7)$$

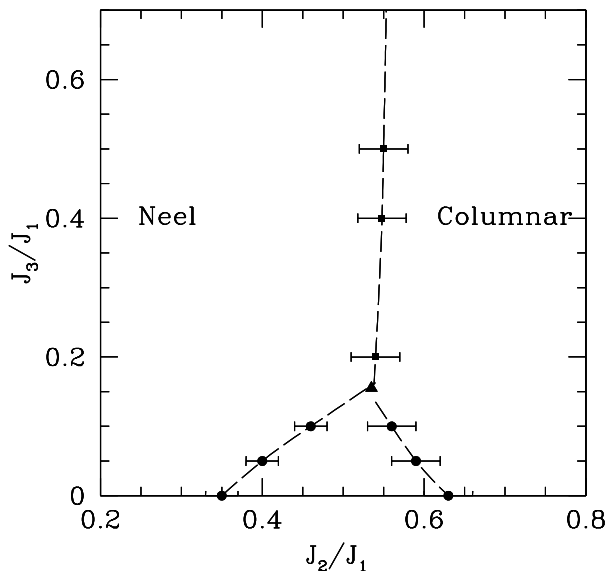


Figure 4: Phase diagram obtained from various series expansions. The dashed lines are first-order transitions, and the filled triangle is a triple point.

Here the notations $(1x)$ and $(1y)$ refer to nearest neighbor J_1 bonds in the x and y direction in a plane, respectively. We have calculated the expansion to order λ^8 inclusive, involving a total of 114650 distinct clusters with 4 types of bond.

C. Results

Series were computed and analysed for the cases $J_3 = 0, 0.05, 0.1, 0.2, 0.5, 1.0$ and a range of values of J_2 in both

the Néel and columnar phases. We set $J_1 = 1$ throughout.

Figure 2 shows estimates of the ground state energy per site versus J_2 for two cases, $J_3 = 0$ (Fig.2a) and $J_3 = 1.0$ (Fig.2b). The energy is evaluated by forming Padé approximants to the series and evaluating these at $\lambda = 1$. Error bars, where shown, represent confidence limits, based on the degree of consistency between high-order approximants.

As is apparent, the behaviour of the energy estimates is quite different in the two cases. For $J_3 = 0$, i.e the $J_1 - J_2$ square lattice model, the energy estimates in the intermediate range $J_2 = (0.4, 0.6)$ become erratic and the two curves, from the Néel and columnar series respectively, do not appear to join. However, for $J_3 = 1$, the estimates are quite precise and the two curves cross near $J_2 \simeq 0.55$. The clear difference in slope of the two branches at the crossing point indicates a direct first-order transition between the two phases.

To analyse the magnetization series we first performed a Huse transformation [21] to a new variable $x = 1 - \sqrt{1 - \lambda}$ to remove the square-root singularity at $\lambda = 1$, expected from spin-wave theory. This procedure has been used in earlier work on the 2D antiferromagnet [21, 22]. Padé approximants to the new series were then evaluated at $x = 1$.

The results are shown in Figure 3 and again display a striking difference between the two cases $J_3 = 0$ and $J_3 = 1$. For $J_3 = 0$ we see clear evidence of an intermediate non-magnetic phase, with Néel and columnar magnetizations vanishing near $J_2 \simeq 0.4$ and $J_2 \simeq 0.6$ respectively. The error bars are large near the transition points and it is not possible to say whether the transitions are first- or second-order. It is generally believed that the columnar-disordered transition is first-order while the Néel-disordered transition appears second-order but may, in fact, be weakly first-order [15]. On the other hand, for

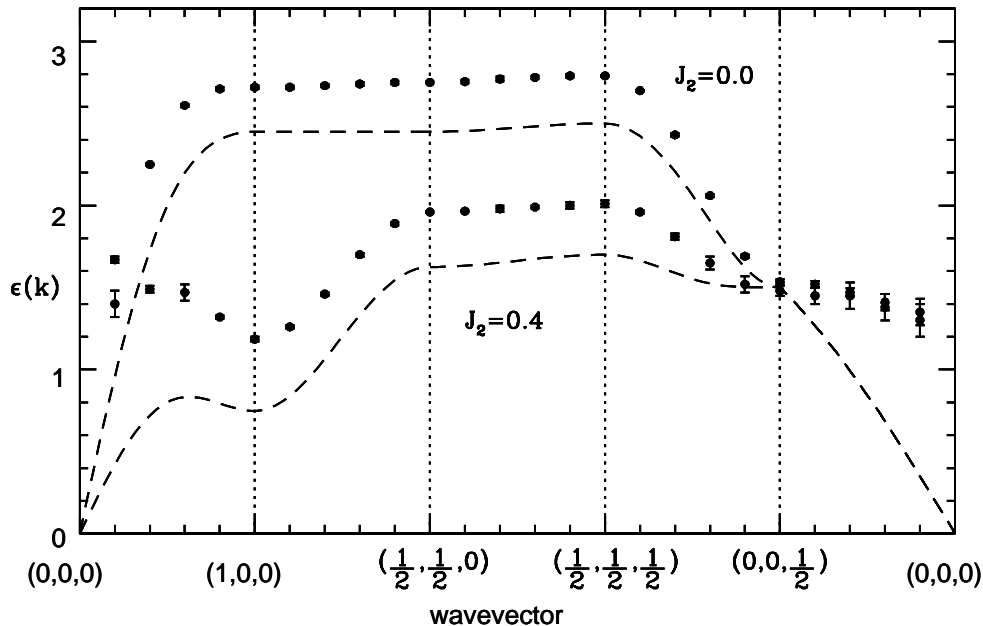


Figure 5: Series estimates of the single-magnon dispersion relations in the Néel phase at $J_2/J_1 = 0.0$, $J_3/J_1 = 0.5$ (upper curve), and $J_2/J_1 = 0.4$, $J_3/J_1 = 0.5$ (lower curve). The dashed lines are linear spin-wave predictions. Values of $\mathbf{q} = \mathbf{k}/\pi$ along the path are shown at the bottom.

$J_3 = 1$ (Fig.3b) it is clear that both magnetizations remain finite throughout their phase. This is consistent with a direct first-order transition.

Proceeding in this way with other values of J_3 , we construct a phase diagram as shown in Figure 4, which confirms the schematic phase diagram in Figure 1b. As is apparent, the disordered phase narrows as the interplane coupling J_3 is increased, and vanishes at the estimated point $J_2/J_1 = 0.54 \pm 0.03$, $J_3/J_1 = 0.16 \pm 0.03$. This value of J_3 is a little lower than found previously [16].

III. EXCITATIONS

It is also of interest to investigate the spectrum of single-magnon excitations in the ordered phases and to see how these change on increasing the interlayer coupling J_3 . Standard series methods exist for calculating the excitation energy throughout the Brillouin zone [17], and we utilize these in the following.

A. Néel Phase

Series were obtained to order λ^7 , based on 255196 distinct clusters of up to 8 sites. In Fig. 5 we show dispersion curves for two values of the frustrating interaction

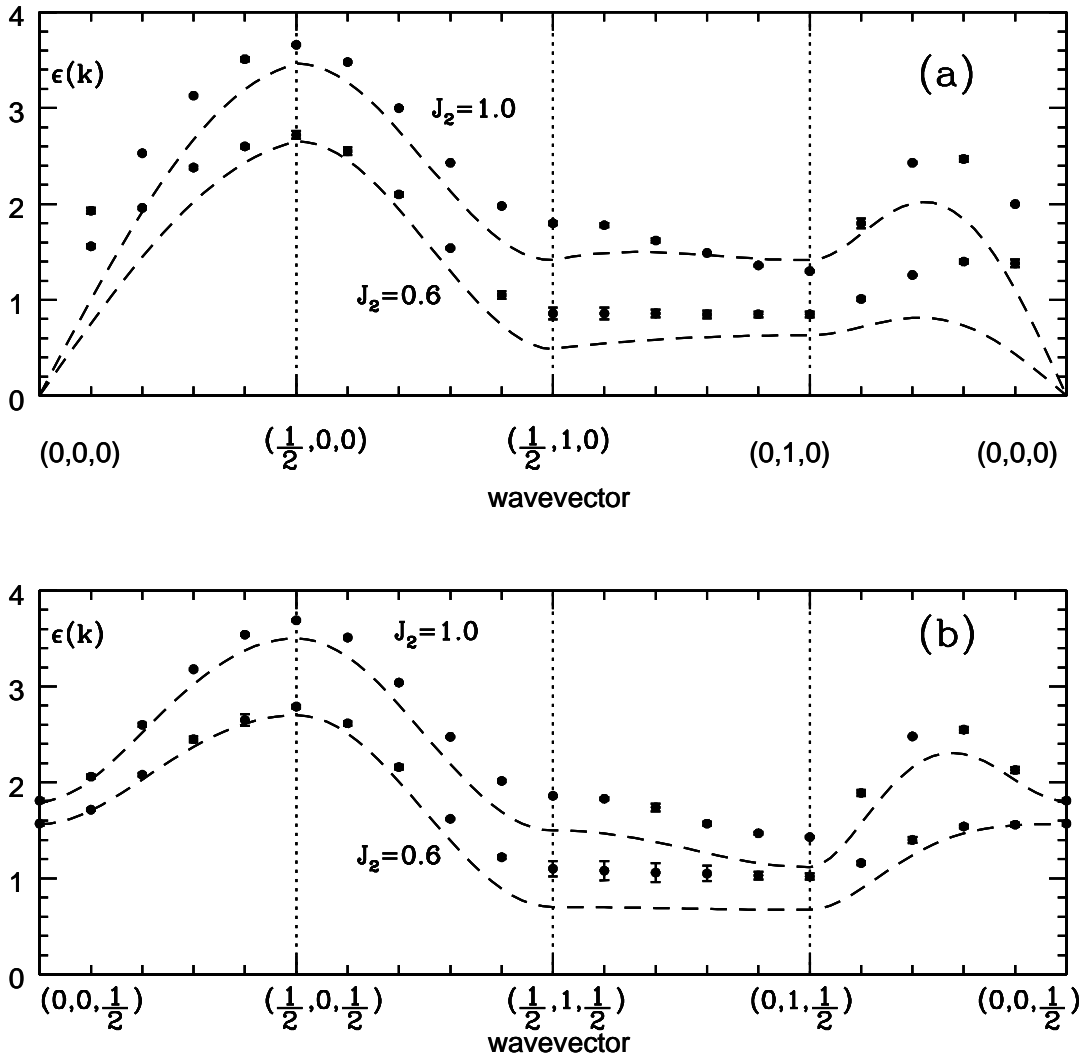


Figure 6: Series estimates of the single-magnon dispersion relations in the columnar phase at (a) $J_2/J_1 = 1.0$, $J_3/J_1 = 0.5$, $k_z = 0$ (upper curve) and $J_2/J_1 = 0.6$, $J_3/J_1 = 0.5$, $k_z = 0$ (lower curve), and (b) $J_2/J_1 = 1.0$, $J_3/J_1 = 0.5$, $k_z = \pi/2$ (upper curve) and $J_2/J_1 = 0.6$, $J_3/J_1 = 0.5$, $k_z = \pi/2$ (lower curve). The dashed lines are linear spin-wave predictions. Values of $\mathbf{q} = \mathbf{k}/\pi$ along the path are shown at the bottom.

$J_2 = 0.0, 0.4$ for $J_3 = 0.5$, along various symmetry lines in the Brillouin zone, as shown. For comparison we also show the results of linear spin-wave theory.

Several features are worth noting:

- (1) A very pronounced dip develops at wavevector $(\pi, 0, 0)$ (and, by symmetry, also at $(0, \pi, 0)$) with increasing J_2 . Linear spin-wave theory has the gap vanishing at $J_2 = 0.5$ (see Appendix).
- (2) There is a distinct ‘shoulder’ at $(0, 0, \pi/2)$, which is not seen in linear spin-wave theory. Indeed, along

the whole line $(0, 0, k_z)$ the energy depends only weakly on J_2 .

- (3) Linear spin-wave theory reproduces the overall dispersion curves reasonably well, but systematically underestimates the excitation energies.

We note also that the series become very irregular near the Goldstone point $\mathbf{k} = \mathbf{0}$, and the Padé approximants do not accurately show the vanishing of the gap at this point. This has been noted in previous work [23], and an indirect way found to overcome this problem, which also

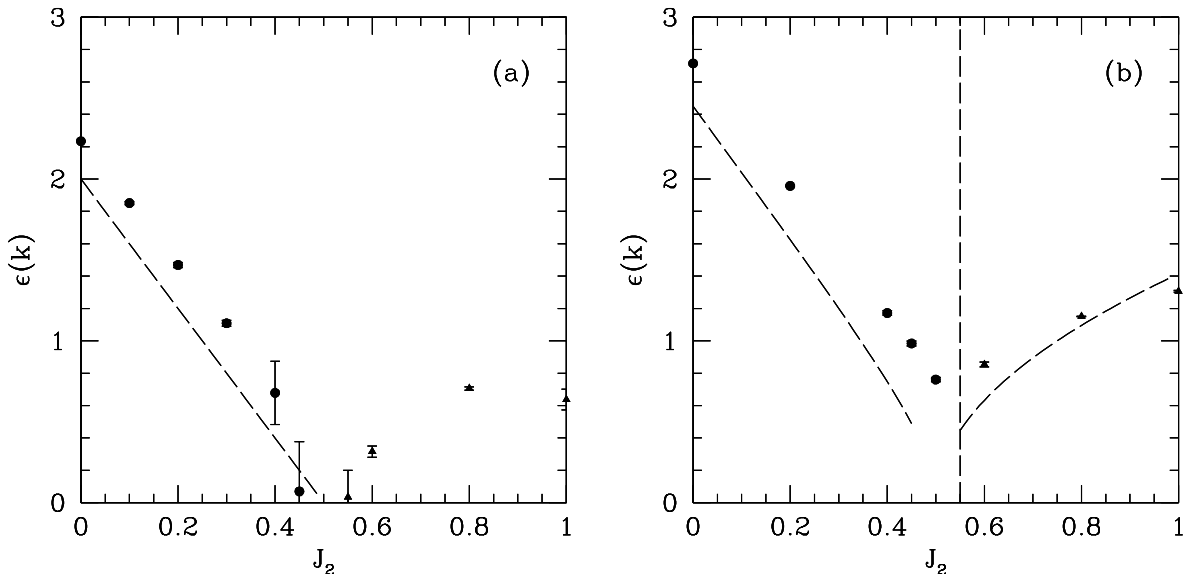


Figure 7: Series estimates of the energy gap $\epsilon(\mathbf{k})$ at $\mathbf{k} = (0, \pi, 0)$ as a function of J_2 at (a) $J_3 = 0$ and (b) $J_3 = 0.5$. Filled circles - Néel phase; filled triangles - columnar phase. The dashed lines are linear spin-wave predictions in each phase.

allows calculation of the spin-wave velocity. However, we do not address this further in the present work.

B. Columnar Phase

Series were obtained to order λ^7 , based on 490487 distinct clusters with up to 8 sites, and 4 possible bond types. In Figure 6 we show dispersion curves for $J_3 = 0.5$ and $J_2 = 1.0, 0.6$ along various symmetry lines in the Brillouin zone. The predictions of linear spin-wave theory are shown as dashed lines.

The most notable feature is the depressed excitation energy along the line $(\pi/2, \pi, 0)$ to $(0, \pi, 0)$. The dispersion curve in this region flattens as J_2 decreases from 1.0 to 0.6, in both cases (a) and (b). According to linear spin-wave theory this whole branch becomes soft at $J_2/J_1 = 0.5$, the classical transition point. Again linear spin-wave theory tends to underestimate the excitation energy, but not as badly as for the Néel phase. The same difficulty with the Goldstone point $\mathbf{k} = \mathbf{0}$, discussed above for the Néel phase, occurs here.

C. The Energy Gap at $(0, \pi, 0)$

As the phase transition is approached, from either the Néel or columnar side, we expect increasing quantum fluctuations at wavevector $\mathbf{k} = (0, \pi, 0)$, which should be manifest through a decreasing energy gap at this point. As mentioned above, linear spin-wave theory predicts a vanishing excitation energy at this \mathbf{k} point at the classical transition point $J_2/J_1 = 0.5$. Hence the variation

of the gap is of some interest, and our results are shown in Figure 7, as a function of J_2 , for two values of the coupling ratio $J_3/J_1 = 0, 0.5$.

In the case $J_3/J_1 = 0.5$ (Fig. 7b) the gaps remain of substantial size right up to the direct first-order transition, and the gaps appear to be of roughly equal magnitude in both phases at the transition. This is a further sign that the transition between the two ordered phases is first order at this value of J_3 .

Figure 7a shows the energy gap at $J_3 = 0$. Note that whereas linear spin wave theory has the gap vanishing at all couplings in the columnar phase, it is in fact finite at larger J_2 , as given by a modified spin-wave theory and earlier series results [13]. Note also that the energy gaps in both phases extrapolate to zero before reaching the classical transition point $J_2/J_1 = 0.5$, providing further evidence of a disordered intermediate phase when $J_3 = 0$. Taken at face value, the results indicate that the gap remains finite at the estimated transition points $J_2 \simeq 0.4$ and $J_2 \simeq 0.6$, which would indicate first order transitions. Naive extrapolations are not entirely reliable near a critical point, however, and a more precise check of this point would be of interest. A Dlog Padé analysis of the series in λ gives no consistent estimates of the critical point in this case.

IV. CONCLUSIONS

We have used series expansion methods to study a system of stacked $J_1 - J_2$ layers with antiferromagnetic coupling J_3 between the layers. This model is applicable to the layered materials $\text{Li}_2\text{VO}_2\text{SiO}_4$ and $\text{Li}_2\text{VOGeO}_4$, as

well as being of intrinsic theoretical interest. In agreement with earlier work of Schmalfluss *et al.* [16], we find that the disordered region of the phase diagram becomes narrower as J_3 is increased, and vanishes completely at a triple point, beyond which there is a direct first-order transition between the Néel and columnar phases. We estimate the location of the triple-point as $J_2/J_1 = 0.54 \pm 0.03$, $J_3/J_1 = 0.16 \pm 0.03$, the J_3 value being somewhat lower than in ref. [16].

As well as mapping out the phase ground state phase diagram, we have computed magnon dispersion curves along symmetry lines in the Brillouin zone, in both the Néel and columnar phases, for various parameter values. This would allow a more critical evaluation of the validity of the model for the materials mentioned above, when experimental inelastic neutron scattering results for magnon energies become available.

After this work had been completed we became aware of two other recent studies of this model. Nunes *et al.* [24], using an effective field theory approach, concluded that the triple point (they refer to this as a critical end-point, assuming the Néel to disordered transition is second order) lies at $J_2/J_1 = 0.56$, $J_3/J_1 = 0.67$, values much higher than obtained in the present work and in other work [16, 20]. Majumdar [25] has carried out a spin-wave calculation to second order ($1/S^2$) and concludes that the intermediate phase remains present even at $J_3 = 1$, which seems surprising in view of the other work referred to above.

Finally we mention another recent study [26] of a different generalization of the 2-dimensional $J_1 - J_2$ model,

in which the frustrating J_2 interactions are included in all spatial directions. That model appears also to have an interesting phase diagram, and could be studied by series methods.

V. ACKNOWLEDGEMENTS

We are grateful for the computing resources provided by the Australian Partnership for Advanced Computing (APAC) National Facility.

Appendix A: Linear Spin-Wave Theory

In the Appendix we present the results of linear spin-wave theory (LSWT) for the model, for both the Néel and columnar phases. The results have been used in the main text to compare with the more accurate series results.

The basic procedures of LSWT are well known so we will not include all details.

1. Néel Phase

There are two equivalent sublattices A, B and two sets of bosons describing spin deviations from the classical Néel state. After Fourier transformation the Hamiltonian is, to quadratic order

$$\begin{aligned}
 H = & -NS^2(2J_1 - 2J_2 + J_3) + 2S(2J_1 - 2J_2 + J_3) \sum_k (a_k^\dagger a_k + b_k^\dagger b_k) \\
 & + 4SJ_1 \sum_k \gamma_k (a_k^\dagger b_k^\dagger + a_k b_k) + 4SJ_2 \sum_k \mu_k (a_k^\dagger a_k + b_k^\dagger b_k) + 2SJ_3 \sum_k \nu_k (a_k^\dagger b_k^\dagger + a_k b_k)
 \end{aligned} \quad (\text{A1})$$

with

$$\gamma_k = \frac{1}{2}(\cos k_x + \cos k_y), \mu_k = \cos k_x \cos k_y, \nu_k = \cos k_z \quad (\text{A2})$$

This is then diagonalized by a standard Bogoliubov transformation, yielding

$$H = E_0 + \sum_k \omega_k (A_k^\dagger A_k + B_k^\dagger B_k) \quad (\text{A3})$$

with

$$\begin{aligned}
 \omega_k &= 2S\sqrt{P_k^2 - Q_k^2} \\
 P_k &= 2J_1 + J_3 - 2J_2(1 - \mu_k) \\
 Q_k &= 2J_1\gamma_k + J_3\nu_k
 \end{aligned} \quad (\text{A4})$$

The ground state energy is

$$E_0 = -NS(S+1)(2J_1 - 2J_2 + J_3) + \sum_k \omega_k \quad (\text{A5})$$

and the sublattice magnetization is

$$M = S + \frac{1}{2} - \frac{2S}{N} \sum_k \frac{P_k}{\omega_k} \quad (\text{A6})$$

We note that for small k

$$\begin{aligned}
 P_k + Q_k &= 2(2J_1 + J_3) - \frac{1}{2}(J_1 + 2J_2)(k_x^2 + k_y^2) \\
 &\quad - \frac{1}{2}J_3k_z^2 + \dots \\
 P_k - Q_k &= \left(\frac{1}{2}J_1 - J_2\right)(k_x^2 + k_y^2) + \frac{1}{2}J_3k_z^2 + \dots
 \end{aligned} \quad (\text{A7})$$

so there is a linear Goldstone mode at $\mathbf{k} = 0$, provided $J_2 < J_1/2$. The phase becomes unstable for $J_2 \geq J_1/2$.

Another special case occurs at $\mathbf{k} = (\pi, 0, 0)$. Let $\mathbf{k}' = \mathbf{k} - (\pi, 0, 0)$ be small, then

$$\begin{aligned} P_k + Q_k &= 2J_1 - 4J_2 + \frac{J_3}{2}k'_z{}^2 + J_2(k'_x{}^2 + k'_y{}^2) + \dots \\ P_k - Q_k &= 2J_1 - 4J_2 + 2J_3 + J_2(k'_x{}^2 + k'_y{}^2) \\ &\quad - \frac{J_3}{2}k'_z{}^2 + \dots \end{aligned} \quad (\text{A8})$$

Hence the gap at $\mathbf{k}' = 0$ vanishes at $J_2 = J_1/2$, regardless of J_3 , corresponding to a phase transition.

2. Columnar Phase

There are again two sublattices, with the A and B sites forming successive columns. The Fourier transformed Hamiltonian is now

$$\begin{aligned} H &= -NS^2(2J_2 + J_3) + 2S \sum_k (J_1 \cos k_y + 2J_2 + J_3)(a_k^\dagger a_k + b_k^\dagger b_k) \\ &\quad + 2S \sum_k (J_1 \cos k_x + 2J_2 \mu_k + J_3 \nu_k)(a_k^\dagger b_k^\dagger + a_k b_k) \end{aligned} \quad (\text{A9})$$

A Bogoliubov transformation then yields

$$H = E_0 + \sum_k \omega_k (A_k^\dagger A_k + B_k^\dagger B_k) \quad (\text{A10})$$

with

$$E_0 = -NS(S+1)(2J_2 + J_3) + \sum_k \omega_k \quad (\text{A11})$$

and

$$\begin{aligned} \omega_k &= 2S \sqrt{P_k^2 - Q_k^2} \\ P_k &= J_1 \cos k_y + 2J_2 + J_3 \\ Q_k &= J_1 \cos k_x + 2J_2 \cos k_x \cos k_y \\ &\quad + J_3 \cos k_z \end{aligned} \quad (\text{A12})$$

The sublattice magnetization is again given by the formula (A6).

For small k

$$\begin{aligned} P_k - Q_k &= \frac{1}{2}(J_1 + 2J_2)k_x^2 + \frac{1}{2}(2J_2 - J_1)k_y^2 \\ &\quad + \frac{1}{2}J_3k_z^2 + \dots \end{aligned} \quad (\text{A13})$$

which shows that again there is a Goldstone mode at $\mathbf{k} = \mathbf{0}$, which is stable for $J_2 > J_1/2$, but becomes unstable at $J_2 = J_1/2$.

Another special case is $\mathbf{k} = (k_x, \pi, 0)$, when

$$P_k - Q_k = (2J_2 - J_1)(1 + \cos k_x) + \dots \quad (\text{A14})$$

Hence ω_k vanishes along this line at $J_2 = J_1/2$, corresponding again to the transition point.

-
- [1] P. Chandra and B. Doucot, Phys. Rev. B **38**, 9335 (1988).
 - [2] E. Dagotto and A. Moreo, Phys. Rev. Lett. **63**, 2148 (1989).
 - [3] H.J. Schulz and T.A.L. Ziman, Europhys. Lett. **18**, 355 (1992); H.J. Schulz, T.A.L. Ziman and D. Poilblanc, J. Phys. **16**, 675 (1996).
 - [4] J. Richter, Phys. Rev. B **47**, 5794 (1993); J. Richter, N.B. Ivanov and K. Retzlaff, Europhys. Lett. **25**, 545 (1994).
 - [5] J. Oitmaa and Zheng Weihong, Phys. Rev. B **54**, 3022 (1996).
 - [6] R.F. Bishop, D.J.J. Farnell and J.B. Parkinson, Phys. Rev. B **58**, 6394 (1998).
 - [7] R.R.P. Singh, Zheng Weihong, C.J. Hamer and J. Oitmaa, Phys. Rev. B **60**, 7278 (1999).
 - [8] L. Capriotti and S. Sorella, Phys. Rev. Lett. **84**, 3173 (2000).
 - [9] L. Siurakshina, D. Ihle and R. Hayn, Phys. Rev. B **64**, 104406 (2001).
 - [10] O. P. Sushkov, J. Oitmaa and Z. Weihong, Phys. Rev. B **63**, 104420 (2001).
 - [11] L. Capriotti, F. Becca, A. Parola and S. Sorella, Phys. Rev. Lett. **87**, 097201 (2001).
 - [12] L. Capriotti, F. Becca, A., Parola, A., and S. Sorella, Phys. Rev. B **67**, 212402 (2003).
 - [13] R.R.P. Singh, Weihong Zheng, J. Oitmaa, O.P. Sushkov and C.J. Hamer, Phys. Rev. Lett. **91**, 017201 (2003).
 - [14] T. Roscilde, A. Feiguin, A.L. Chernyshev, S. Liu and S. Haas, Phys. Rev. Lett. **93**, 017203 (2004).
 - [15] J. Sirker, Z. Weihong, O. P. Sushkov and J. Oitmaa, Phys. Rev. B **73**, 184420 (2006).

- [16] D. Schmalfuss, R. Darradi, J. Richter, J. Schulenberg and D. Ihle, Phys. Rev. Lett. **97**, 157201 (2006).
- [17] J. Oitmaa, C. J. Hamer and Z. Weihong, *Series Expansion Methods for Strongly Interacting Lattice Models*, Cambridge, (2006)
- [18] H. Rosner, R. R. P. Singh, W. H. Zheng, J. Oitmaa, S.-L. Drechsler and W. E. Pickett, Phys. Rev. Lett. **88**, 186405 (2002); H. Rosner, R. R. P. Singh, W. H. Zheng, J. Oitmaa, and W. E. Pickett, Phys. Rev. B **67**, 014416 (2003).
- [19] G. S. Uhrig, M. Holt, J. Oitmaa, O. P. Sushkov, and R. R. P. Singh, Phys. Rev. B **79**, 092416 (2009).
- [20] M. Holt, O.P. Sushkov, D. Stanek and G.S. Uhrig, preprint arXiv:1010.5551v1 (2010)
- [21] D. A. Huse, Phys. Rev. B **37**, 2380 (1988).
- [22] Zheng Weihong, J. Oitmaa and C.J. Hamer, Phys. Rev. B **43**, 8321 (1991).
- [23] R.R.P. Singh, Phys. Rev. B **47**, 12337 (1993); R.R.P. Singh and M.P. Gelfand, *ibid.* **52**, R15695 (1995).
- [24] W. A. Nunes, J. Ricardo de Sousa, J. Roberto Viana and J. Richter, J. Phys. Cond. Mat. **22**, 146004 (2010).
- [25] K. Majumdar, J. Phys. Cond. Mat. **23**, 046001 (2011).
- [26] K. Majumdar and T. Datta, J. Stat. Phys. **139**, 714 (2010).